



DOCKET

07-AFC-6

DATE JAN 29 2010

RECD. JAN 29 2010

500 Capitol Mall, Suite 1600
Sacramento, California 95814
main 916.447.0700
fax 916.447.4781
www.stoel.com

JOHN A. MCKINSEY
Direct (916) 319-4746
jamckinsey@stoel.com

January 29, 2010

Mr. Paul Kramer, Hearing Officer
California Energy Commission
1516 Ninth Street
Sacramento, CA 95814

Re: Carlsbad Energy Center Project (07-AFC-6)

Dear Mr. Kramer:

Applicant Carlsbad Energy Center LLC ("Applicant") herein respectfully requests that the following documents be added as exhibits to Applicant's Rebuttal Testimony:

- Exhibit 190: Revised Plot Plan re Secondary Access (cited in Applicant's Rebuttal Testimony; inadvertently missed during duplication of Rebuttal Exhibits 110-189)
- Exhibit 191: Reclaimed Water Email Correspondence
- Exhibit 192: Rebuttal Greenhouse Gas Exhibit
- Exhibit 193: Water Non-Availability Letter, dated February 20, 2008 (cited in City's Testimony; not identified as exhibit)



Mr. Paul Kramer, Hearing Officer
January 29, 2010
Page 2

Exhibit 190 was referred to in Applicant's Rebuttal Testimony, but was inadvertently not submitted with other exhibits. Exhibit 193 is a letter relied upon in the City of Carlsbad's Opening Testimony, but not included as an exhibit. This letter was previously docketed with the Energy Commission (Docket #45467) and served upon all parties. (*See* Testimony of Joe Garuba at p. 14.) Exhibits 191 and 192 were identified as relevant to Applicant's rebuttal testimony concerning water resources and greenhouse gases as a result of discussions at the Prehearing Conference concerning topics for cross-examination and topics of particular interest to the Committee.

Very truly yours,

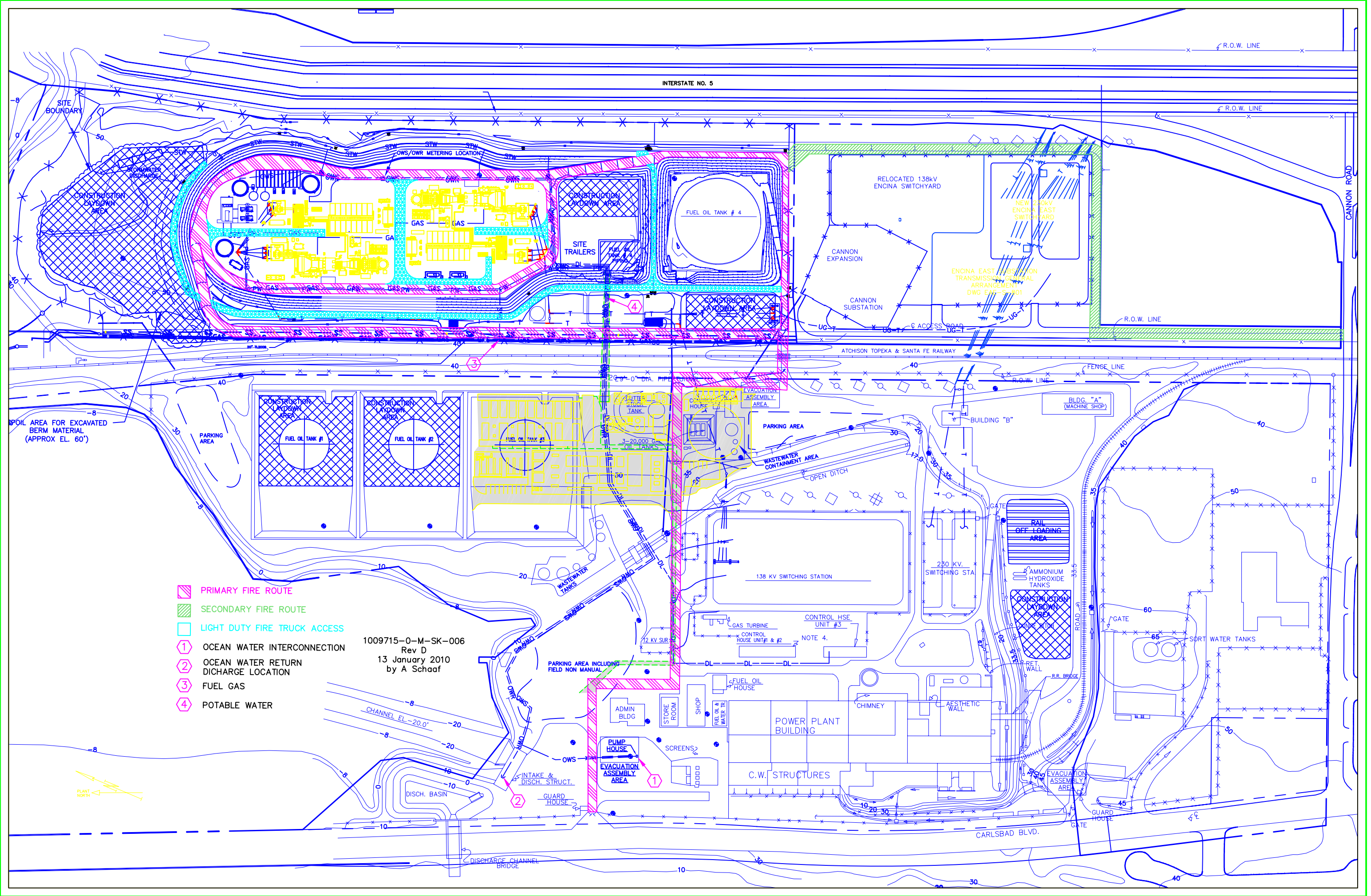

John A. McKinsey


JAM:adc

cc: See Attached Proof of Service

Enclosures

EXHIBIT 190



- PRIMARY FIRE ROUTE
- SECONDARY FIRE ROUTE
- LIGHT DUTY FIRE TRUCK ACCESS
- 1 OCEAN WATER INTERCONNECTION
- 2 OCEAN WATER RETURN DISCHARGE LOCATION
- 3 FUEL GAS
- 4 POTABLE WATER

1009715-0-M-SK-006
 Rev D
 13 January 2010
 by A Schaaf



INTERSTATE NO. 5

R.O.W. LINE

R.O.W. LINE

CANNON ROAD

R.O.W. LINE

ATCHISON TOPEKA & SANTA FE RAILWAY

FENCE LINE

R.O.W. LINE

SPOIL AREA FOR EXCAVATED BERM MATERIAL (APPROX EL. 60')

PARKING AREA

FUEL OIL TANK #1

FUEL OIL TANK #2

FUEL OIL TANK #3

3-20,000 GALS OIL TANKS

EVACUATION ASSEMBLY AREA

PARKING AREA

WASTEWATER CONTAINMENT AREA

OPEN DITCH

BLDG. "A" (MACHINE SHOP)

BUILDING "B"

RAIL OFF-LOADING AREA

AMMONIUM HYDROXIDE TANKS

CONSTRUCTION LAYDOWN AREA

RET. WALL

R.R. BRIDGE

WATER TANKS

GATE

GATE

GATE

GATE

PARKING AREA INCLUDING FIELD NON MANUAL

ADMIN BLDG

STORE ROOM

SHOP

FUEL OIL HOUSE

POWER PLANT BUILDING

CHIMNEY

AFESTHETIC WALL

C.W. STRUCTURES

EVACUATION ASSEMBLY AREA

GUARD HOUSE

CHANNEL EL. -20.0'

DISCH. BASIN

DISCHARGE CHANNEL BRIDGE

INTAKE & DISCH. STRUCT.

GUARD HOUSE

EXHIBIT 191

Bob Wojcik

From: Terry Smith [TSmit@ci.carlsbad.ca.us]
Sent: Tuesday, July 10, 2007 12:12 PM
To: Bob Wojcik
Cc: Bill Plummer
Subject: Re: Reclaimed Water Line at Power Plant

Attachments: 70001479.tif



70001479.tif (634
KB)

Bob,

Here is a copy of the drawing of the recycled water line in Cannon Road at Avenida Encinas. You will need to talk to Bill about the other issue, but I would be surprised if we could get it done faster than a private company. Also, if it is going to be a public line, we would have to pay prevailing wage to the contractor and would presumably expect full reimbursement from NRG for this line.

Terry

>>> "Bob Wojcik" <bobw@hofmanplanning.com> 07/03/2007 2:08 PM >>>

Hi Bill and Terry,

(Bill, I had left you a voice mail about this earlier today.)

I need to get a copy of a plan\drawing that shows where to nearest reclaimed water line is\will be to serve the power plant site. Would you please let me know how I can obtain a copy of that plan? My current understanding is that there is a line at Avenida Encinas and Cannon Road.

We would like to get confirmation as to whether the City will construct a new reclaimed water line north from Cannon Road on to the plant site. This was discussed at the meeting we had at NRG's offices in May. Because of the intervening private property, between Cannon Road and NRG's site, it was considered more expedient for the city to either use an existing easement across that property or obtain a public easement.

Please let me know what the city has decided about this.

Happy Fourth of July!

Bob Wojcik

Director of Engineering

Hofman Planning and Engineering

5900 Pasteur Court Suite 150

Carlsbad, Ca. 92008

(760) 438-1465

bobw@hofmanplanning.com

Bob Wojcik

From: Bill Plummer [Bplum@ci.carlsbad.ca.us]
Sent: Friday, July 27, 2007 1:05 PM
To: Bob Wojcik
Cc: David Ahles; Eva Plajzer; Terry Smith
Subject: Re: Reclaimed Water Line at Power Plant

The drawing showing the 24" recycled transmission main is designed by CMWD shown on sheet 3 , Cannon road Recycled Water Transmission Main and South Agua Hedionda Interceptor Sewer dated 5-3-98. CMWD 88-602 and 92-406. It is DMS under Cannon. It is CML&C steel thickness 0.1563" CLASS 200. It is in Cannon Road and then turns south onto Avenida Encinas.. You will need to connect to this pipeline and extend it to the location of the new power plant. CMWD would not be able to fund the pipe extension. Pressure is from our 384 Pressure zone. Ground elevation appears to be around 50' therefore available static pressure is around 145 psi to 150 psi. We received the request for will serve letter and will place the projected water demand in our H2ONET model. The pipeline extension can be placed in an existing easement if we have the clearances needed.

>>> "Bob Wojcik" <bobw@hofmanplanning.com> 07/03/2007 2:08 PM >>>

Hi Bill and Terry,

(Bill, I had left you a voice mail about this earlier today.)

I need to get a copy of a plan\drawing that shows where to nearest reclaimed water line is\will be to serve the power plant site. Would you please let me know how I can obtain a copy of that plan? My current understanding is that there is a line at Avenida Encinas and Cannon Road.

We would like to get confirmation as to whether the City will construct a new reclaimed water line north from Cannon Road on to the plant site. This was discussed at the meeting we had at NRG's offices in May. Because of the intervening private property, between Cannon Road and NRG's site, it was considered more expedient for the city to either use an existing easement across that property or obtain a public easement.

Please let me know what the city has decided about this.

Happy Fourth of July!

Bob Wojcik

Director of Engineering

Hofman Planning and Engineering

5900 Pasteur Court Suite 150

Carlsbad, Ca. 92008

(760) 438-1465

bobw@hofmanplanning.com

Bob Wojcik

From: Bill Plummer [Bplum@ci.carlsbad.ca.us]
Sent: Monday, August 06, 2007 1:34 PM
To: Bob Wojcik
Subject: Re: NRG "Will Serve" Letter

Bob: We typically do issue will serve letters. I am working on a response but there are some issues. I am sending them a letter today.

>>> "Bob Wojcik" <bobw@hofmanplanning.com> 08/06/2007 1:30 PM >>>

Hi Bill,

NRG has asked if we could obtain a "will serve" letter from the City for sewer, water and reclaimed water. I realize that the City typically does not issue such letters, however, NRG needs them as a part of their permit processing with other governmental agencies.

Would you please let me know how we can get these?

Thanks, Bob

Bob Wojcik

Director of Engineering

Hofman Planning and Engineering

5900 Pasteur Court Suite 150

Carlsbad, Ca. 92008

(760) 438-1465

bobw@hofmanplanning.com

-----Original Message-----

From: Bill Plummer [mailto:Bplum@ci.carlsbad.ca.us]

Sent: Tuesday, December 04, 2007 5:40 PM

To: Doyle, Chris

Subject: Re: Meeting Today

Chris: I have been directed to have you work through Joe Garuba located at the City Manger's office for future work on this approach or any others for water supply. His telephone number is 434-2893

>>> "Doyle, Chris" <Chris.Doyle@nrgenergy.com> 12/04/2007 8:05 AM >>>
Bill,

Either that or a long term contact so the City could justify doing it itself. If I buy/own the equipment, how would we address if you use it for other customers? Either way sounds like a plan. I would like to meet with you and the Plant Manager to discuss the best way to do this from an engineering/operations perspective..

Thanks,

Chris

----- Original Message -----

From: Bill Plummer <Bplum@ci.carlsbad.ca.us>

To: Doyle, Chris

Sent: Tue Dec 04 10:49:25 2007

Subject: RE: Meeting Today

Chris: If NRG was willing to develop a microfiltration/reverse osmosis (MF/RO) plant at our site we could furnish all the water you would need. The treated water would be delivered through a dedicated pipeline extending from our plant to the power plant. This would assume NRG pays for the plant, the O&M cost and a replacement fund to replace membranes, pumps, etc. If interested let me know and I will pursue this on my end.

>>> "Doyle, Chris" <Chris.Doyle@nrgenergy.com> 12/03/2007 4:33 PM >>>
Bill,

Thanks again for meeting with me today. I will follow up with you near the end of the week.

Thanks,

Chris

-----Original Message-----

From: Bill Plummer [mailto:Bplum@ci.carlsbad.ca.us]

Sent: Monday, December 03, 2007 9:51 AM

To: Doyle, Chris

Subject: Re: Meeting Today

1635 faraday ave.

>>> "Doyle, Chris" <Chris.Doyle@nrgenergy.com> 12/03/2007 7:20 AM >>>

Bill,

I just wanted to confirm your office is on Faraday.

Thanks,

Chris

EXHIBIT 192



On the determination of climate feedbacks from ERBE data

Richard S. Lindzen¹ and Yong-Sang Choi¹

Received 16 June 2009; revised 14 July 2009; accepted 20 July 2009; published 26 August 2009.

[1] Climate feedbacks are estimated from fluctuations in the outgoing radiation budget from the latest version of Earth Radiation Budget Experiment (ERBE) nonscanner data. It appears, for the entire tropics, the observed outgoing radiation fluxes increase with the increase in sea surface temperatures (SSTs). The observed behavior of radiation fluxes implies negative feedback processes associated with relatively low climate sensitivity. This is the opposite of the behavior of 11 atmospheric models forced by the same SSTs. Therefore, the models display much higher climate sensitivity than is inferred from ERBE, though it is difficult to pin down such high sensitivities with any precision. Results also show, the feedback in ERBE is mostly from shortwave radiation while the feedback in the models is mostly from longwave radiation. Although such a test does not distinguish the mechanisms, this is important since the inconsistency of climate feedbacks constitutes a very fundamental problem in climate prediction. **Citation:** Lindzen, R. S., and Y.-S. Choi (2009), On the determination of climate feedbacks from ERBE data, *Geophys. Res. Lett.*, 36, L16705, doi:10.1029/2009GL039628.

1. Introduction

[2] The purpose of the present note is to inquire whether observations of the earth's radiation imbalance can be used to infer feedbacks and climate sensitivity. Such an approach has, as we will see, some difficulties, but it appears that they can be overcome. This is important since most current estimates of climate sensitivity are based on global climate model (GCM) results, and these obviously need observational testing.

[3] To see what one particular difficulty is, consider the following conceptual situation: We instantaneously double CO₂. This will cause the characteristic emission level to rise to a colder level with an associated diminution of outgoing longwave radiation (OLR). The resulting radiative imbalance is what is generally referred to as radiative forcing. However, the resulting warming will eventually eliminate the radiative imbalance as the system approaches equilibrium. The actual amount of warming associated with equilibration as well as the response time will depend on the climate feedbacks in the system. These feedbacks arise from the dependence of radiatively important substances like water vapor (which is a powerful greenhouse gas) and clouds (which are important for both infrared and visible radiation) on the temperature. If the feedbacks are positive, then both the equilibrium warming and the response time will increase; if they are negative,

both will decrease. Simple calculations as well as GCM results suggest response times on the order of decades for positive feedbacks and years or less for negative feedbacks [Lindzen and Giannitsis, 1998, and references therein]. The main point of this example is to illustrate that the climate system tends to eliminate radiative imbalances with characteristic response times.

[4] Now, in 2002–2004 several papers noted that there was interdecadal change in the top-of-atmosphere (TOA) radiative balance associated with a warming between the 1980's and 1990's [Chen *et al.*, 2002; Wang *et al.*, 2002; Wielicki *et al.*, 2002a, 2002b; Cess and Udelhofen, 2003; Hatzidimitriou *et al.*, 2004; Lin *et al.*, 2004]. Chou and Lindzen [2005] inferred from the interdecadal changes in net radiation at TOA and surface temperature that there was a strong negative feedback. However, this result was internally inconsistent since the persistence of the imbalance over a decade implied a positive feedback. A subsequent correction to the satellite data eliminated much of the decadal variation in the radiative balance [Wong *et al.*, 2006].

[5] However, it also made clear that one could not readily use decadal variability in surface temperature to infer feedbacks from observed radiation data. Rather one needs to look at temperature variations that are long compared to the time scales associated with the feedback processes, but short compared to the response time over which the system equilibrates. This is also important so as to unambiguously observe changes in the radiative budget that are responses to fluctuations in SST as opposed to changes in SST resulting from changes in the radiative budget; the latter will occur on the response time of the system. The primary feedbacks involving water vapor and clouds occur on time scales of days [Lindzen *et al.*, 2001; Rodwell and Palmer, 2007], while response times for relatively strong negative feedbacks remain on the order of a year [Lindzen and Giannitsis, 1998, and references therein]. That said, it is evident that, because the system attempts to restore equilibrium, there will be a tendency to underestimate negative feedbacks relative to positive feedbacks that are associated with longer response times.

2. Data and Analysis

[6] The observed data used in this study are the 16-year (1985–1999) monthly record of the sea surface temperatures (SSTs) from the National Centers for Environmental Prediction, and the Earth radiation budget from the Earth Radiation Budget Experiment (ERBE) [Barkstrom, 1984] nonscanner edition 3 dataset. Note that this data were recently altitude-corrected and are acknowledged to be stable long-term climate dataset based on broadband flux measurements [Wong *et al.*, 2006]. The data can provide reasonably reliable evidence of fluctuations in the anomalies of SST, OLR, and reflected shortwave radiation (SWR) from the tropical means

¹Program in Atmospheres, Oceans, and Climate, Massachusetts Institute of Technology, Cambridge, Massachusetts, USA.

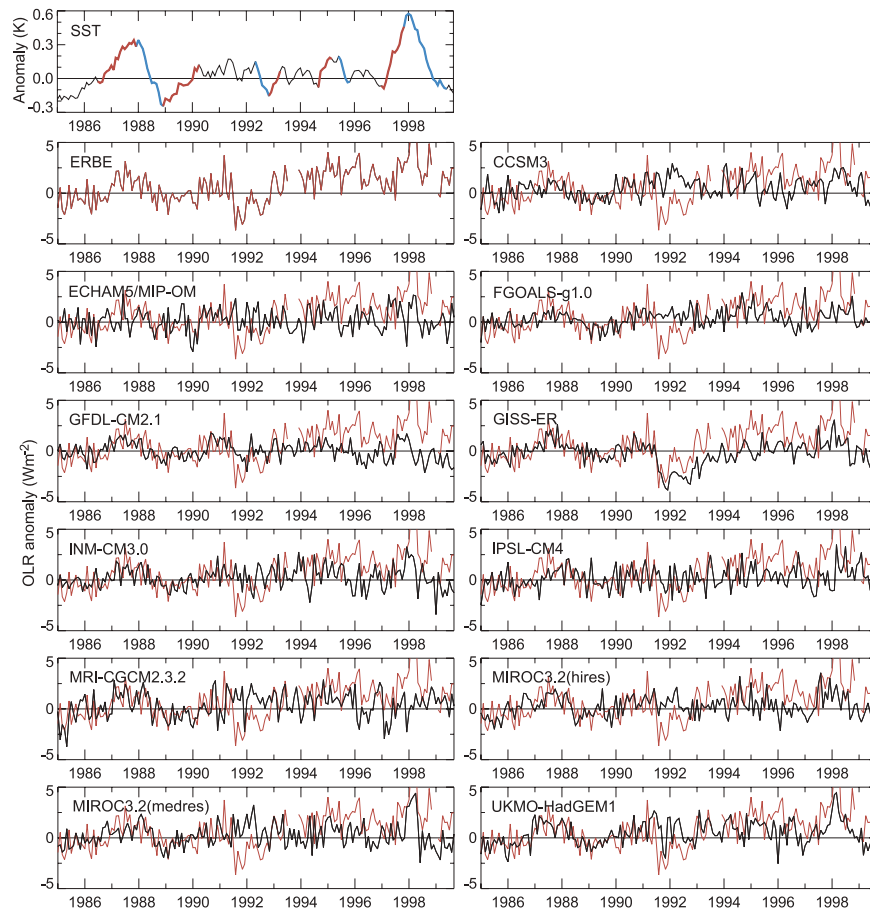


Figure 1a. Monthly SST, and TOA OLR from ERBE (red) and AMIP models (black) for 20°S – 20°N . The major SST intervals for which ΔSST exceeds 0.2°C are indicated by red and blue colors.

(20°S – 20°N); the anomalies are deseasonalized by the monthly means for the period of 1985 through 1989 for the purpose of comparison with climate models [Wielicki *et al.*, 2002a, 2002b]. The effect of land temperature (22% of the whole tropics) on the tropical radiation budget could not be taken into account in this study, due to limited satellite retrievals of surface temperature over the land [Chou and Lindzen, 2005].

[7] The anomalies include a semiannual signal due to the temporal aliasing effect that needs to be eliminated [Trenberth, 2002]. The relevant sampling error of the tropical monthly ERBE data is about 1.7 W m^{-2} for SWR and 0.4 W m^{-2} for OLR [Wielicki *et al.*, 2002a, 2002b]. This spurious signal, particularly in the SWR, can be removed in a 36-day average, reducing the SWR error to the order of 0.3 W m^{-2} . However, in this study, the 36-day average was not applied because we wish to relate monthly SSTs to monthly ERBE TOA fluxes. Instead, the moving average with a 7-month smoother was used for the SWR anomalies alone; however, we will see that the smoothing does not much affect the main results. With respect to instrumental stability, the nonscanner records agree relatively well with the scanner records for the period from 1985 to 1989, but no longer agree with them as well for the later period (difference of up to 3 W m^{-2}) [Wong *et al.*, 2006]. The fundamental difference between the two types of radiometers comes from the fact that, while the nonscanner views the entire hemisphere of radiation, the scanner views radiance from a single direction and estimates the

hemispheric emission or reflection [Wielicki *et al.*, 2002a]. It is difficult to quantify possible influences due to this difference, but the present study requires only short term stability and this may be less affected.

[8] The analysis was also made for the model TOA fluxes. The atmospheric model intercomparison projects (AMIP) program for the 4th Assessment Report of the Intergovernmental Panel on Climate Change (IPCC-AR4) provides model results for atmospheric GCMs forced by observed SSTs. AMIP also provides the equilibrium climate sensitivity for the models included [Intergovernmental Panel on Climate Change, 2007].

[9] The next obvious question is whether fluctuations with the time scales associated with feedback processes exist in the observed data and models. Figures 1a and 1b show that such fluctuations (ΔFlux) are amply available in OLR and SWR, although data are not currently available in some periods in 1993 and 1999. However, it is possible that many of the very small fluctuations are simply noise. Restricting oneself to fluctuations in SST (ΔSST) which exceed 0.2 K still leaves nine cases in the available data (red and blue lines in Figure 1a). Note that appreciable fluctuations of the anomalies are due to El Niño events (in 1982/83, 1986/87, 1991/92, and 1997/98), La Niña events (in 1988/90), and Pinatubo eruption (in 1991) [Wielicki *et al.*, 2002a; Wong *et al.*, 2006].

[10] Figure 2 compares estimates of net $\Delta\text{Flux}/\Delta\text{SST}$ for intervals for which ΔSST exceeded 0.1 K ; the net flux is calculated for OLR + SWR. Results are shown both for 11

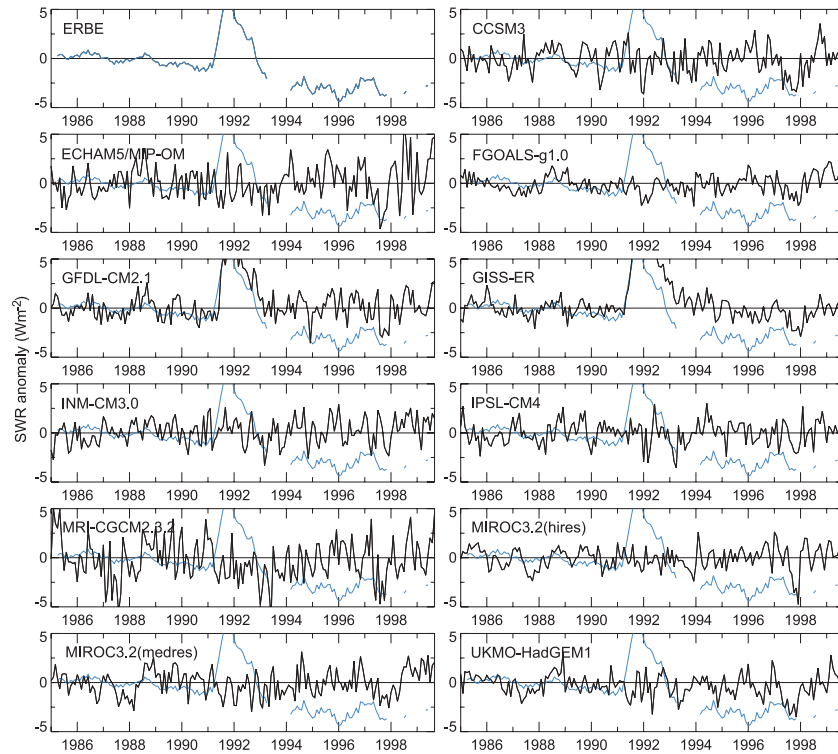


Figure 1b. The same as Figure 1a but for reflected shortwave radiation from ERBE (blue) and AMIP models (black).

AMIP models, and for the ERBE data. ERBE has a positive $\Delta\text{Flux}/\Delta\text{SST}$, whereas all models have a negative $\Delta\text{Flux}/\Delta\text{SST}$. Table 1 compares net $\Delta\text{Flux}/\Delta\text{SST}$ for intervals for which ΔSST exceeded 0.1, 0.2 K, . . . , for 3, 5, and 7 month time smoothing, for all monthly intervals. We see that all provide essentially the same result, but that scatter is significantly reduced by using threshold 0.2 K without time

smoothing. One may take $\Delta\text{Flux}/\Delta\text{SST}$ with one month intervals, and secure more than hundred cases (Table 1). However, unless we confine ΔSST to exceed 0.1 K, the inclusion of what is essentially noise leads to an increase in scatter, and statistically insignificant $\Delta\text{Flux}/\Delta\text{SST}$. In addition, based on the known uncertainty of ERBE data, it is expected that uncertainty in $\Delta\text{Flux}/\Delta\text{SST}$ for $\Delta\text{SST} \geq 0.2$ K

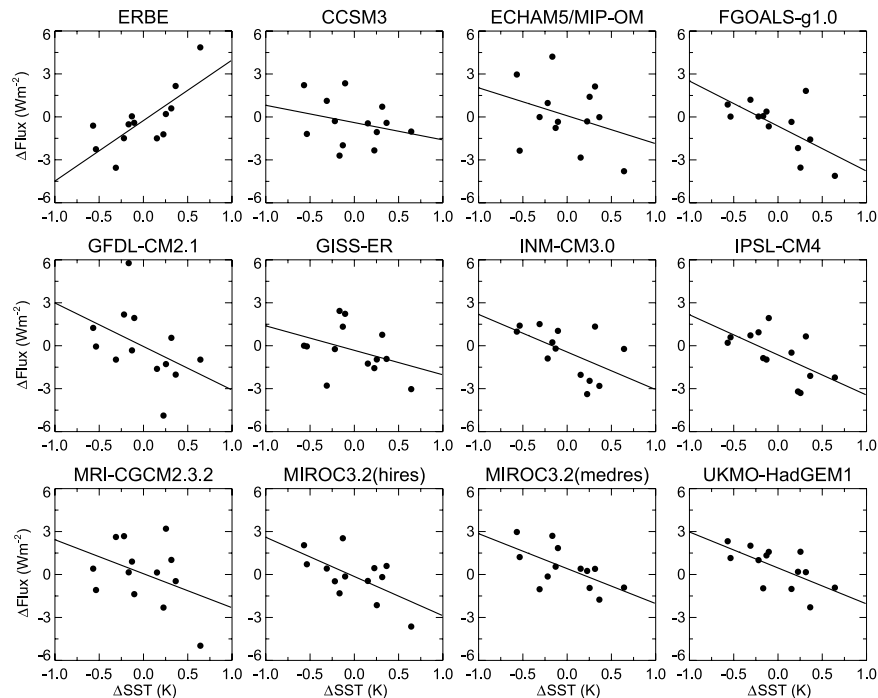


Figure 2. Scatterplots of net ΔFlux against ΔSST for ERBE and models. Plots for ΔSST exceeds 0.1°C are displayed.

Table 1. Regression Statistics Between Net ΔFlux and ΔSST and Standard Errors of Net $\Delta\text{Flux}/\Delta\text{SST}$ for ERBE and Models^a

Case	Number	Slope	ERBE		Models		SE
			R	SE	Slope	R	
0.1 K, Unfiltered	13	4.23	0.74	1.54	-2.41	-0.49	2.4
0.2 K, Unfiltered	9	4.55	0.79	1.63	-2.33	-0.53	1.76
0.3 K, Unfiltered	6	5.02	0.86	1.57	-2.00	-0.58	1.49
0.4 K, Unfiltered	3	5.24	0.97	1.87	-2.62	-0.88	1.54
0.1 K, 3 months	5	5.36	0.82	2.21	-2.14	-0.64	1.46
0.1 K, 5 months	4	7.98	0.78	5.09	-1.60	-0.34	2.02
0.1 K, 7 months	4	9.26	0.93	1.83	-1.50	-0.20	3.39
0.2 K, 3 months	4	6.01	0.90	2.36	-1.99	-0.61	1.33
0.2 K, 5 months	3	11.40	0.95	6.89	-2.73	-0.49	1.82
Monthly interval	176	1.29	0.03	19.78	-1.66	-0.06	14.81
0.05 K, Monthly	54	0.56	0.02	4.58	-2.10	-0.11	2.76
0.1 K, Monthly	6	1.90	0.15	5.02	-4.64	-0.30	5.03

^aSWR is filtered with 7-month smoother in all cases.

is up to 1.5 and 2 $\text{W m}^{-2} \text{K}^{-1}$ for the shortwave (SW) and longwave (LW) fluxes, respectively. That said, the opposite signal between ERBE and the models is hardly attributable to observational errors. Note that we will next show that $\Delta\text{Flux}/\Delta\text{SST}$ is a measure of the feedback factor for the climate system.

[11] Following *Chou and Lindzen* [2005] and *Lindzen et al.* [2001], we use the following equation to relate $\Delta\text{Flux}/\Delta\text{SST}$ to equilibrium climate sensitivity. In the nonfeedback climate, climate sensitivity is defined as the response of temperature ΔT_0 to an external forcing ΔQ :

$$\Delta T_0 = G_0 \Delta Q, \quad (1)$$

where G_0 is a nonfeedback gain. The mean OLR in the whole tropics is approximately 255 W m^{-2} [*Barkstrom*, 1984], and is equivalent to an effective emitting temperature of 259 K. Thus G_0 is calculated by the inverse of the derivative of the Planck function with respect to the temperature at 259 K; $G_0 \approx 0.25 \text{ W}^{-1} \text{ m}^2 \text{ K}$. For a doubling of CO_2 ($\Delta Q \approx 3.7 \text{ W m}^{-2}$), ΔT_0 is $\sim 0.925 \text{ K}$ ($= 0.25 \times 3.7$).

[12] In the presence of feedback processes, an additional forcing proportional to the response ΔT (i.e., $F\Delta T$) is provided to ΔQ in equation (1). The response is now

$$\Delta T = G_0(\Delta Q + F\Delta T), \quad (2)$$

and

$$\Delta T = \frac{\Delta T_0}{1-f}, \quad (3)$$

where $f = G_0 F$ is the feedback factor. The net feedback is positive for $0 < f < 1$, and negative for $f < 0$. The feedback parameter F is $-\Delta\text{Flux}/\Delta\text{SST}$, assuming the same incoming radiation in the system. The negative sign pertains because increased outgoing flux means energy loss. For example, with $\Delta\text{SST} = 0.2 \text{ K}$ and $\Delta\text{Flux} = 0.9 \text{ W m}^{-2}$, F is $-4.5 \text{ W m}^{-2} \text{K}^{-1}$ ($= -0.9/0.2$) that is equivalent to $f = -1.1$, resulting in ΔT of $\sim 0.5 \text{ K}$ for a doubling of CO_2 in equation (3). Namely, given $F = -4.5 \text{ W m}^{-2} \text{K}^{-1}$, climate sensitivity is about a half of that for the nonfeedback condition. On the other hand, negative $\Delta\text{Flux}/\Delta\text{SST}$ is equivalent to climate sensitivity for a doubling of CO_2 higher than 1 K. All models agree as to positive feedback, and all models disagree very

sharply with the observations. However, it is difficult to accurately determine sensitivity from $\Delta\text{Flux}/\Delta\text{SST}$ from the models. Varying $\Delta\text{Flux}/\Delta\text{SST}$ values even slightly by 1 $\text{W m}^{-2} \text{K}^{-1}$, which can simply be a measurement error [*Wong et al.*, 2006], climate sensitivity for a doubling of CO_2 can have any value higher than 1 K. For example, the 2 K to 4.5 K is the likelihood range of climate sensitivity in IPCC-AR4, which corresponds to $\Delta\text{Flux}/\Delta\text{SST} = -2.3$ to $-3.3 \text{ W m}^{-2} \text{K}^{-1}$. Similar explanation on why climate sensitivity is so unpredictable is given by *Roe and Baker* [2007].

[13] When considering LW and SW fluxes separately, F is replaced by $F_{\text{LW}} + F_{\text{SW}}$. In the observed $\Delta\text{OLR}/\Delta\text{SST}$, the nonfeedback change of 4 $\text{W m}^{-2} \text{K}^{-1}$ is included. Also $\Delta\text{SWR}/\Delta\text{SST}$ needs to be balanced with $\Delta\text{OLR}/\Delta\text{SST}$. From the consideration, $F_{\text{LW}} = -\Delta\text{OLR}/\Delta\text{SST} + 4$ and $F_{\text{SW}} = -\Delta\text{SWR}/\Delta\text{SST} - 4$. In the case of no SW feedback ($F_{\text{SW}} = 0$), $\Delta\text{OLR}/\Delta\text{SST}$ less than 4 $\text{W m}^{-2} \text{K}^{-1}$ represents positive feedback; $\Delta\text{OLR}/\Delta\text{SST}$ more than 4 $\text{W m}^{-2} \text{K}^{-1}$ represents negative feedback; $\Delta\text{OLR}/\Delta\text{SST}$ less than 0 $\text{W m}^{-2} \text{K}^{-1}$ represents infinite feedback, which is physically unreal.

3. Concluding Remarks

[14] In Figure 3, we see that ERBE and model results differ substantially. In Figures 3a and 3b, we evaluate equation (3) using ΔFlux for only OLR and only SWR. The curves are for the condition assuming no SW feedback and assuming no LW feedback in panels a and b, respectively. In panel a, model results fall on the curve given by equation (3), because the model average of SW feedbacks is almost zero. In Figure 3b, models with smaller LW feedbacks are closer to the curve for no LW feedback; the model results would lie on the curve assuming positive LW feedback. When in Figure 3c we consider the total flux (i.e., LW + SW), model results do lie on the theoretically expected curve. Looking at Figure 3, we note several important features:

[15] 1. The models display much higher climate sensitivity than is inferred from ERBE.

[16] 2. The (negative) feedback in ERBE is mostly from SW while the (positive) feedback in the models is mostly from OLR.

[17] 3. The theoretical relation between $\Delta\text{Flux}/\Delta\text{SST}$ and sensitivity is very flat for sensitivities greater than 2°C . Thus, the data does not readily pin down such sensitivities. This was the basis for the assertion by *Roe and Baker* [2007] that

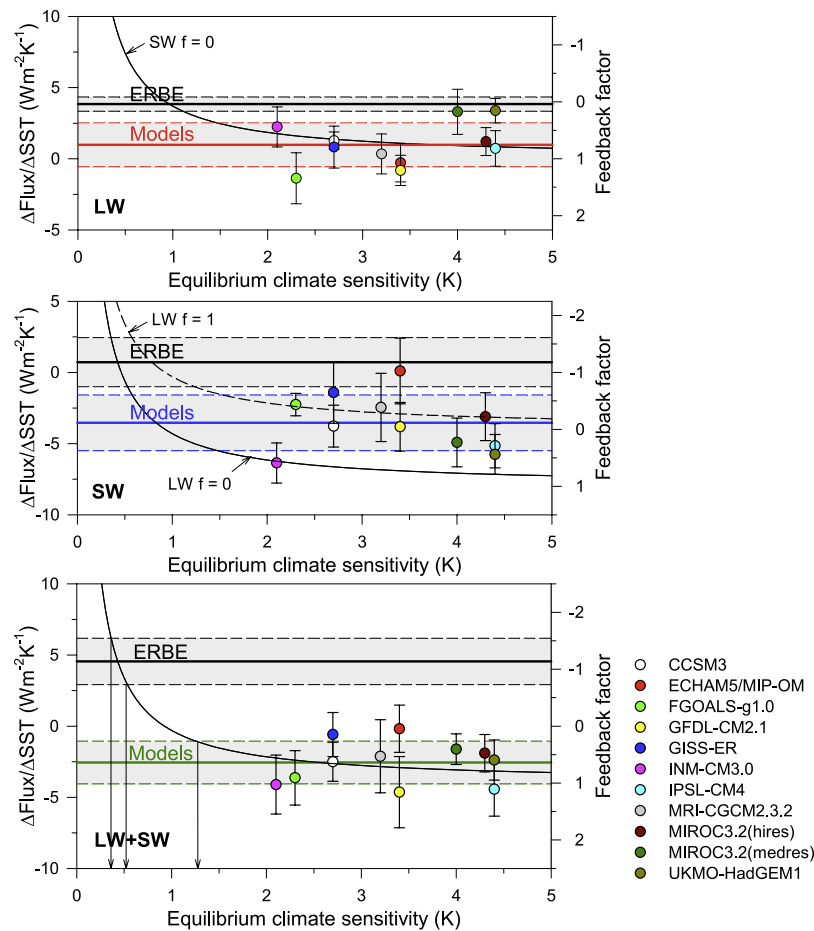


Figure 3. ERBE-observed and AMIP-simulated ratios of (a) LW, (b) SW, and (c) total (LW + SW) radiative flux changes to temperature changes ($\Delta\text{Flux}/\Delta\text{SST}$) with respect to the equilibrium climate sensitivity. The horizontal solid and dashed lines are the mean and the standard error of $\Delta\text{Flux}/\Delta\text{SST}$. The solid curves are theoretical estimate of climate sensitivity for LW feedback under assumption of no SW feedback (Figure 3a), for SW feedback under assumption of no LW feedback (Figure 3b), and for total feedback (Figure 3c).

determination of climate sensitivity was almost impossible [Allen and Frame, 2007]. However, this assertion assumes a large positive feedback. Indeed, Figure 3c suggests that models should have a range of sensitivities extending from about 1.5°C to infinite sensitivity (rather than 5°C as commonly asserted), given the presence of spurious positive feedback. However, response time increases with increasing sensitivity [Lindzen and Giannitsis, 1998], and models were probably not run sufficiently long to realize their full sensitivity. For sensitivities less than 2°C , the data readily distinguish different sensitivities, and ERBE data appear to demonstrate a climate sensitivity of about 0.5°C which is easily distinguished from sensitivities given by models.

[18] Note that while TOA flux data from ERBE are sufficient to determine feedback factors, this data do not specifically identify mechanisms. Thus, the small OLR feedback from ERBE might represent the absence of any OLR feedback; it might also result from the cancellation of a possible positive water vapor feedback due to increased water vapor in the upper troposphere [Soden *et al.*, 2005] and a possible negative iris cloud feedback involving reduced upper level cirrus clouds [Lindzen *et al.*, 2001]. With respect to SW feedbacks, it is currently claimed that model SW

feedbacks are largely associated with the behavior of low level clouds [Bony *et al.*, 2006, and references therein]. Whether this is the case in nature cannot be determined from ERBE TOA observations. However, more recent data from CALIPSO lidar (CALIOP) and CloudStat radar (CPR) do offer height resolution, and we are currently studying such data to resolve the issue of what, in fact, is determining SW feedbacks. Finally, it should be noted that our analysis has only considered the tropics. Following Lindzen *et al.* [2001], allowing for sharing this tropical feedback with neutral higher latitudes could reduce the negative feedback factor by about a factor of two. This would lead to an equilibrium sensitivity that is $2/3$ rather than $1/2$ of the non-feedback value. This, of course, is still a small sensitivity.

[19] **Acknowledgments.** This research was supported by DOE grant DE-FG02-01ER63257 and by the Korea Ministry of Environment. The authors thank NASA Langley Research Center and PCMDI team for the data. We also thank Roberto Rondanelli, Chang-Hoi Ho and an anonymous reviewer for comments.

References

Allen, M. R., and D. J. Frame (2007), Calling off the quest, *Science*, 318, 582–583, doi:10.1126/science.1149988.

- Barkstrom, B. R. (1984), The Earth Radiation Budget Experiment (ERBE), *Bull. Am. Meteorol. Soc.*, *65*, 1170–1185, doi:10.1175/1520-0477(1984)065<1170:TERBE>2.0.CO;2.
- Bony, S., et al. (2006), How well do we understand and evaluate climate change feedback processes?, *J. Clim.*, *19*, 3445–3482, doi:10.1175/JCLI3819.1.
- Cess, R. D., and P. M. Udelhofen (2003), Climate change during 1985–1999: Cloud interactions determined from satellite measurements, *Geophys. Res. Lett.*, *30*(1), 1019, doi:10.1029/2002GL016128.
- Chen, J., B. E. Carlson, and A. D. Del Genio (2002), Evidence for strengthening of the tropical general circulation in the 1990s, *Science*, *295*, 838–841, doi:10.1126/science.1065835.
- Chou, M.-D., and R. S. Lindzen (2005), Comments on “examination of the decadal tropical mean ERBS nonscanner radiation data for the iris hypothesis,” *J. Clim.*, *18*, 2123–2127, doi:10.1175/JCLI3406.1.
- Hatzidimitriou, D., et al. (2004), On the decadal increase in the tropical mean outgoing longwave radiation for the period 1984–2000, *Atmos. Chem. Phys.*, *4*, 1419–1425.
- Intergovernmental Panel on Climate Change (2007), *Climate Change 2007: The Physical Science Basis. Contribution of Working Group I to the Fourth Assessment Report of the Intergovernmental Panel on Climate Change*, edited by S. Solomon et al., Cambridge Univ. Press, Cambridge, U. K.
- Lin, B., T. Wong, B. A. Wielicki, and Y. Hu (2004), Examination of the decadal tropical mean ERBS nonscanner radiation data from the iris hypothesis, *J. Clim.*, *17*, 1239–1246, doi:10.1175/1520-0442(2004)017<1239:EOTDTM>2.0.CO;2.
- Lindzen, R. S., and C. Giannitsis (1998), On the climatic implications of volcanic cooling, *J. Geophys. Res.*, *103*, 5929–5941, doi:10.1029/98JD00125.
- Lindzen, R. S., M.-D. Chou, and A. Y. Hou (2001), Does the Earth have an adaptive iris?, *Bull. Am. Meteorol. Soc.*, *82*, 417–432, doi:10.1175/1520-0477(2001)082<0417:DTEHAA>2.3.CO;2.
- Rodwell, M. J., and T. N. Palmer (2007), Using numerical weather prediction to assess climate models, *Q. J. R. Meteorol. Soc.*, *133*, 129–146, doi:10.1002/qj.23.
- Roe, G. H., and M. B. Baker (2007), Why is climate sensitivity so unpredictable?, *Science*, *318*, 629–632, doi:10.1126/science.1144735.
- Soden, B. J., D. L. Jackson, V. Ramaswamy, M. D. Schwarzkopf, and X. Huang (2005), The radiative signature of upper tropospheric moistening, *Science*, *310*, 841–844, doi:10.1126/science.1115602.
- Trenberth, K. E. (2002), Changes in tropical clouds and radiation, *Science*, *296*, 2095, doi:10.1126/science.296.5576.2095a.
- Wang, P.-H., P. Minnis, B. A. Wielicki, T. Wong, and L. B. Vann (2002), Satellite observations of long-term changes in tropical cloud and outgoing longwave radiation from 1985 to 1998, *Geophys. Res. Lett.*, *29*(10), 1397, doi:10.1029/2001GL014264.
- Wielicki, B. A., et al. (2002a), Evidence for large decadal variability in the tropical mean radiative energy budget, *Science*, *295*, 841–844, doi:10.1126/science.1065837.
- Wielicki, B. A., et al. (2002b), Changes in tropical clouds and radiation: Response, *Science*, *296*, 2095, doi:10.1126/science.296.5576.2095a.
- Wong, T., et al. (2006), Reexamination of the observed decadal variability of the earth radiation budget using altitude-corrected ERBE/ERBS nonscanner WFOV data, *J. Clim.*, *19*, 4028–4040, doi:10.1175/JCLI3838.1.

Y.-S. Choi and R. S. Lindzen, Program in Atmospheres, Oceans, and Climate, Massachusetts Institute of Technology, 77 Massachusetts Avenue, Cambridge, MA 02139, USA. (ysc@mit.edu)



Cloud and radiation budget changes associated with tropical intraseasonal oscillations

Roy W. Spencer,¹ William D. Braswell,¹ John R. Christy,¹ and Justin Hnilo²

Received 15 February 2007; revised 30 March 2007; accepted 16 July 2007; published 9 August 2007.

[1] We explore the daily evolution of tropical intraseasonal oscillations in satellite-observed tropospheric temperature, precipitation, radiative fluxes, and cloud properties. The warm/rainy phase of a composited average of fifteen oscillations is accompanied by a net reduction in radiative input into the ocean-atmosphere system, with longwave heating anomalies transitioning to longwave cooling during the rainy phase. The increase in longwave cooling is traced to decreasing coverage by ice clouds, potentially supporting Lindzen's "infrared iris" hypothesis of climate stabilization. These observations should be considered in the testing of cloud parameterizations in climate models, which remain sources of substantial uncertainty in global warming prediction. **Citation:** Spencer, R. W., W. D. Braswell, J. R. Christy, and J. Hnilo (2007), Cloud and radiation budget changes associated with tropical intraseasonal oscillations, *Geophys. Res. Lett.*, 34, L15707, doi:10.1029/2007GL029698.

1. Introduction

[2] The tropical tropospheric heat budget is dominated by a quasi-equilibrium balance between latent heating in precipitation systems and longwave (infrared) cooling to outer space [e.g., Manabe and Strickler, 1964]. The precipitation systems also produce clouds that both warm the atmosphere through longwave "greenhouse" warming, and cool the surface through shortwave (solar) shading.

[3] While many investigators have found that these two cloud effects mostly cancel in their influence on the tropical ocean-atmosphere system's heat budget [e.g., Kiehl and Ramanathan, 1990; Cess *et al.*, 2001], any imbalance between these two large terms could significantly feed back on global warming [Chou and Lindzen, 2002; Soden and Held, 2006]. This makes accurate convective and cloud parameterizations in General Circulation Models (GCMs) critical for improving confidence in those model's predictions of future warming.

[4] Aires and Rossow [2003] and Stephens [2005] argue that substantial improvements in GCM parameterizations will not be achieved by inferring "feedbacks" from observed monthly, interannual, or even decadal climate variability. Partly because of the difficulty in separating cause and effect in observational data, they recommend the measurement of high time-resolution (e.g., daily) variations in the relationships (sensitivities) between clouds, radiation, tem-

perature, etc., which can then be compared to the same metrics diagnosed from GCMs.

[5] Here we address the observational part of this recommendation by analyzing the daily evolution of a time composite of fifteen tropical intraseasonal oscillations (ISOs) in a variety of satellite-measured variables. While most investigations of these events examine their regional expression over the tropical west Pacific [e.g., Stephens *et al.*, 2004], we will instead analyze larger-scale, tropical oceanic averages in an attempt to better capture both ascending and descending branches of tropical deep convective circulations and hopefully better estimate their net effect on the tropical atmosphere.

2. Data and Analysis Method

[6] Tropical (20°N to 20°S latitude) oceanic averages covering the period 1 March 2000 to 31 December 2005 were analyzed. Tropospheric air temperature estimates (T_a) come from channel 5 of the Advanced Microwave Sounding Unit (AMSU-A) flying on the NOAA-15 polar orbiting satellite (instrument descriptions can be found at <http://www2.ncdc.noaa.gov/docs/klm/html/c1/sec1-1.htm>). AMSU channel 5 (53.596 GHz) measurements approximate the average temperature of a deep layer of the troposphere, with peak sensitivity around 600 mb. There is a small, 4% to 5%, influence on channel 5 from the tropical lower stratosphere and about a 1% contribution from the ocean surface.

[7] Tropical oceanic measurements of rainfall, surface wind speed, total integrated water vapor, and sea surface temperature (SST) come from NASA's Tropical Rainfall Measuring Mission (TRMM) satellite Microwave Imager (TMI), described by Kummerow *et al.* [1998]. The TMI rainfall algorithm is described by Wentz and Spencer [1998], while the non-rainfall products are described by Wentz [1997] and Wentz *et al.* [2000].

[8] Top of the atmosphere (TOA), all-sky and clear-sky outgoing longwave (LW) and reflected shortwave (SW) flux measurements were made by the Terra satellite Clouds and the Earth's Radiant Energy System (CERES) instrument [Wielicki *et al.*, 1996]. These products, taken from the CERES ES4 Terra FM1 Edition 2 dataset, are "ERBE-like", and are meant to provide continuity with NASA's older Earth Radiation Budget Experiment satellite. We applied the "Rev. 1" corrections, reported by the data provider, to the SW data.

[9] Finally, cloud properties are from the Terra Moderate Resolution Imaging Spectroradiometer (MODIS) [Barnes *et al.*, 1998], using the latest daily Collection 5 MOD08_D3 dataset. All of the original product datasets are daily grids, at either 1.0° or 2.5° spatial resolution, except for the TMI

¹Earth System Science Center, University of Alabama in Huntsville, Huntsville, Alabama, USA.

²Lawrence Livermore National Laboratory, Livermore, California, USA.

Table 1. Dates of Maximum Tropospheric Temperature Anomaly in AMSU Channel 5 for Fifteen ISO Events Chosen for Composite Analysis^a

ISO Event	Date of Peak Tropospheric Temperature (T_a)
1	(1 September 2000)
2	12 February 2001
3	4 May 2001
4	(1 July 2001)
5	18 August 2001
6	(24 March 2002)
7	12 May 2002
8	30 June 2002
9	(11 May 2004)
10	(14 June 2004)
11	(18 August 2004)
12	28 February 2005
13	12 June 2005
14	25 July 2005
15	7 September 2005

^aDates in parentheses correspond to ISOs that did not have sufficient data to be included in the composite analysis of MODIS cloud properties.

products which are three-day grids compiled on a daily basis at 0.25° spatial resolution. The AMSU grids of limb-corrected T_a [Spencer and Braswell, 1997] are archived in-house at UAH as part of our monthly routine processing of global tropospheric temperatures [Christy et al., 2003].

[10] We averaged all daily grids into daily zonal averages for the latitude band 20°N to 20°S , oceans only. Any days with less than 80% of the nominal data coverage were interpolated from the surrounding days' averages. All results that follow are for daily anomalies, which were computed by subtracting a 21-day smoothed average annual cycle from the six year time series of daily zonal averages.

[11] From the daily anomalies, we constructed a time-composite of the fifteen strongest ISOs during the six year period of record, requiring each to be at least 40 days from temperature minimum to temperature minimum. Table 1 lists the dates of maximum T_a about which the ISOs were composited. As an example of the ISO signature, Figure 1 shows two satellites' measurements of daily T_a during 2002. The stronger oscillations have about a 40 day time scale, which is typical of these disturbances [e.g., Madden and Julian, 1994].

3. ISO Signals

[12] The composite ISO signatures in T_a , oceanic surface wind speed, integrated water vapor, and SST (Figure 2a) reveal an increase in surface wind speed and water vapor, and a brief but weak warm signal in SST, during the ISO warming phase. The wind speed and water vapor increases imply enhanced oceanic evaporation rates. During the cooling phase, wind speeds and vapor contents decrease. The amplitude of the wind signal is 15% of the tropical average wind speed, while that of the water vapor oscillation is only 1.5% of its average value.

[13] Most of the above-average rainfall occurs during the T_a warming phase (Figure 2b), with an oscillation amplitude about 20% of the mean rain rate, and a shift in the rain rate distribution to heavier rates during the rainy phase of the oscillation.

[14] Variations in the CERES TOA all-sky (cloudy plus clear) SW and LW fluxes (Figure 2c) reveal the expected

increase in reflected SW flux associated with clouds produced by the rain systems. But the transition from negative to positive LW flux anomalies during the period of above-average rainfall is somewhat surprising. To examine how these flux variations relate to rainfall variations, we divided the radiative flux anomalies by the latent heat release anomalies calculated from the "total rain" curve in Figure 2b. The results (Figure 2d) reveal the usual near-cancellation between LW heating and SW cooling, but only early in the ISO rainy phase. The LW anomalies then unexpectedly transition from warming to cooling during the course of the rainy period. That the all-sky LW change is so much larger than the clear-sky LW change suggests a shift in cloud properties, which brings us to the MODIS cloud product analysis.

[15] Due to an incomplete MODIS data record, all anomalies were recomputed using nine of the original fifteen ISOs for which there were MODIS data available (see Table 1). The resulting composite T_a anomaly (Figure 3a) has a signature very similar to that of the fifteen-ISO composite in Figure 2a. The MODIS cloud products revealed three significant changes associated with the ISO. First, the liquid cloud coverage (Figure 3b) approximately follows the rain activity variations seen in Figure 2a and the reflected SW variations in Figure 2c, but with a likely under estimation between lag days -15 to 0 due to obscuration by overlying ice clouds.

[16] Of greater interest, however, is the ice cloud behavior, which has a much stronger influence on LW fluxes than do liquid clouds. A decrease in ice cloud coverage is seen in Figure 3b, which coincides with the increasing LHR-normalized LW flux seen in Figure 2d. Finally, the average cloud top temperature of all (liquid + ice) clouds warms by 2°C to 3°C during the same period (Figure 3c). Since the cloud top temperature reported in the MODIS data product we used is an average for all cloud types, this cloud top warming might simply be the result of the decreasing ice cloud fraction uncovering liquid clouds below. In any event, both of these changes in ice cloud properties are qualita-

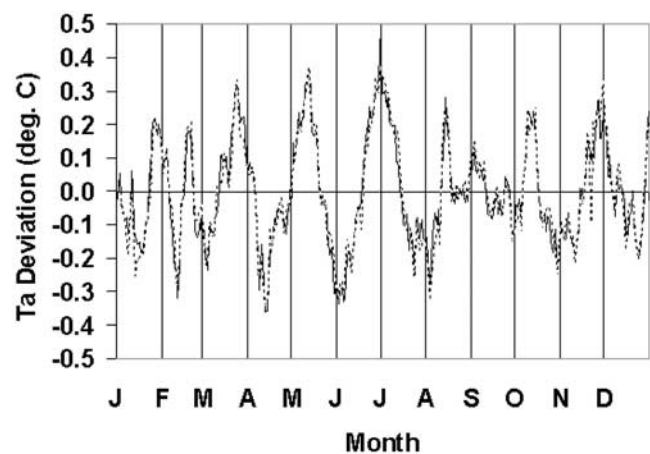


Figure 1. One year of daily tropical average tropospheric temperature from AMSU channel 5 during 2002, solid line is NOAA-15 and dotted line is NOAA-16 satellite. The time series has been high pass filtered to remove time variations longer than intraseasonal.

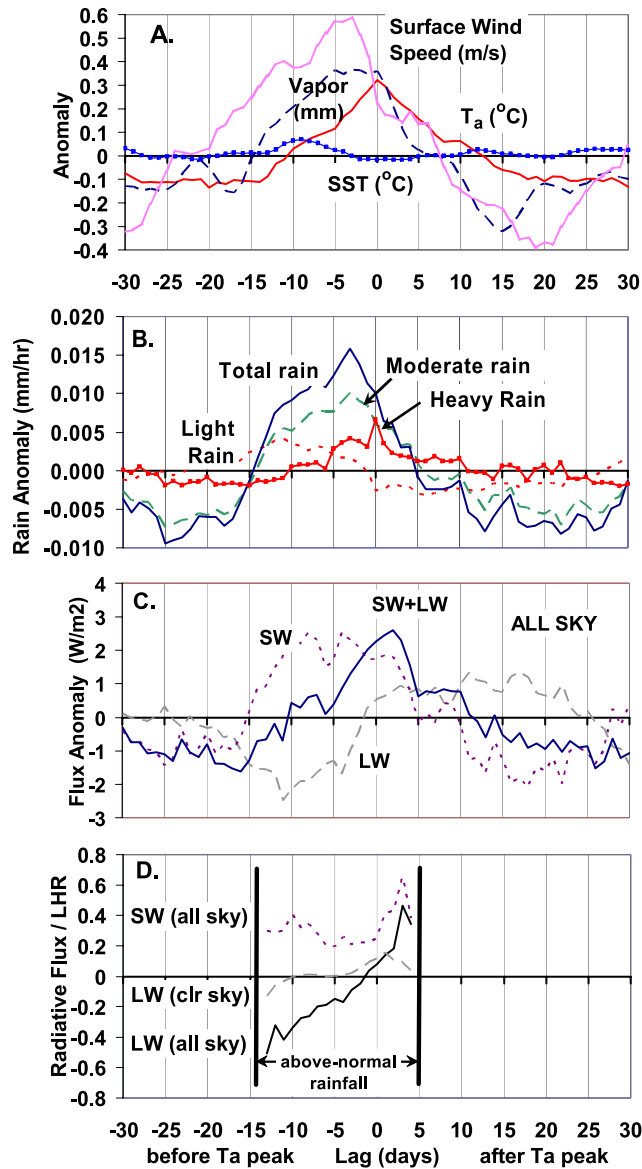


Figure 2. Composite analysis of daily zonal average oceanic anomalies (20°N to 20°S) associated with 15 ISOs, relative to the date of peak tropospheric temperature (T_a): (a) AMSU T_a , and surface wind speed, integrated water vapor, and SST from the TRMM TMI; (b) TMI rain rate; (c): CERES all-sky top-of-atmosphere outgoing longwave (LW) and reflected shortwave (SW) fluxes; (d) CERES fluxes divided by latent heat release calculated from “total rainfall” in Figure 2b.

tively consistent with the all-sky LW transition seen in Figures 2c and 2d.

[17] We estimated the potential effect of the MODIS-observed ice cloud fraction change on the LW flux from

$$\Delta LW = (f_2 - f_1)(LW_{ice} - LW_{no-ice}) \quad (1)$$

where f_1 and f_2 are ice cloud fractions during the warming and cooling phases of the ISO, respectively; LW_{ice} is the ice cloud flux; and LW_{no-ice} is the flux from the remaining areas. With a MODIS-observed decrease in ice cloud

fraction from 0.208 ten days before, to 0.184 ten days after the peak in T_a , and assuming average ice cloud and non-ice cloud LW fluxes of 200 and 285 $W m^{-2}$ (respectively, that we estimated from frequency distributions of all CERES LW data), we estimate a LW flux increase of around 2.0 $W m^{-2}$. This is roughly consistent with the 2.5 $W m^{-2}$ CERES-measured increase in LW flux seen in Figures 2c and 2d during the ISO rainy phase.

[18] The decrease in ice cloud coverage is conceptually consistent with the “infrared iris” hypothesized by *Lindzen et al.* [2001], who proposed that tropical cirroform cloud coverage might open and close, like the iris of an eye, in response to anomalously warm or cool conditions, providing a negative radiative feedback on temperature change. We caution, though, that the ice cloud reduction with tropospheric warming reported here is on a time scale of weeks; it is not obvious whether similar behavior would

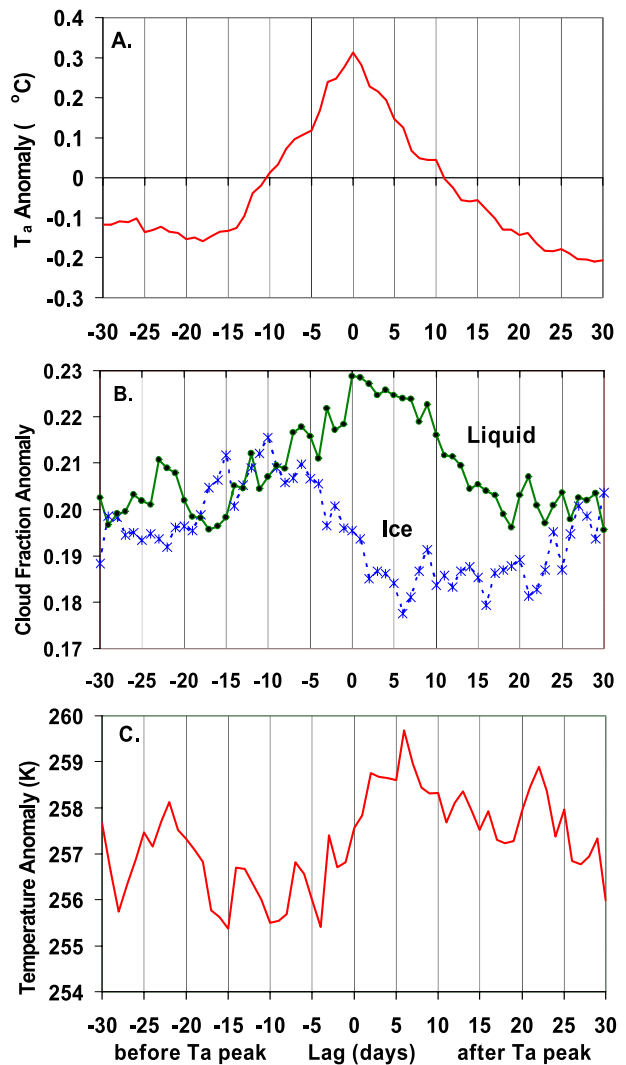


Figure 3. As in Figure 2 but for a composite of nine ISO’s: (a) tropospheric temperature, (b) MODIS liquid and ice cloud fractions, and (c) cloud top temperature (all clouds). The tropical average cloud fraction and cloud top temperature have been added to the anomalies in Figures 3b and 3c.

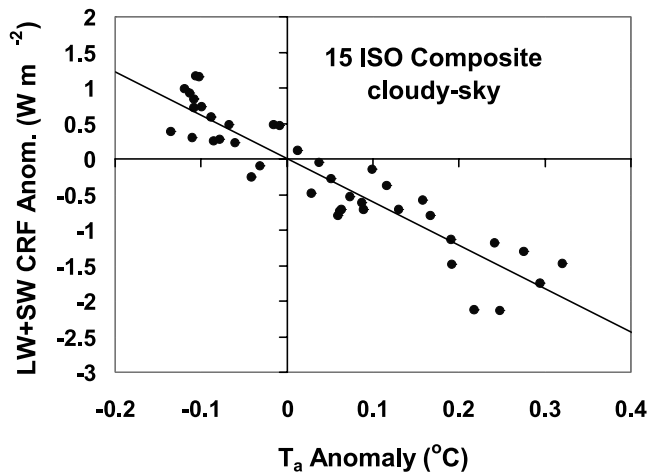


Figure 4. The sum of SW and LW cloud radiative forcings (CRF) versus tropospheric temperature for the 15-ISO composite, which represents about 30% of the six-year data record.

occur on the longer time scales associated with global warming.

[19] We also computed the sensitivity relationships between T_a and the cloud portion of the SW and LW radiative fluxes, which should be of use for comparing to the high time resolution behavior exhibited by climate models. The cloud radiative forcing (CRF), can be defined [e.g., Cess *et al.*, 2001] as:

$$\text{SWCRF} = -(\text{SW}_{\text{all}} - \text{SW}_{\text{clr}}) \quad (2)$$

$$\text{and } \text{LWCRF} = -(\text{LW}_{\text{all}} - \text{LW}_{\text{clr}}), \quad (3)$$

where the sign convention now changes so that positive values of CRF represent heating (flux input), and in our case all quantities are anomalies (deviations from average). The clear-sky SW anomalies (not shown) were small, and are believed to be due to residual cloud contamination in the ERBE methods for identifying clear sky (B. Wielicki, personal communication, 2007). Therefore, the all-sky SW will be assumed to also represent the SW cloud radiative forcing ($\text{SW CRF} \approx -\text{SW}_{\text{all}}$). The clear sky LW anomalies (not shown) were also small (as can be gleaned from Figure 2d), but are still included in our computation of the LW CRF.

[20] The sum of SW CRF ($\approx -\text{SW}_{\text{all}}$) and LW CRF ($= -[\text{LW}_{\text{all}} - \text{LW}_{\text{clr}}]$) plotted against the tropospheric temperature anomalies for the middle 41 days of the fifteen-ISO composite (Figure 4) reveals a strongly negative relationship. A linear regression yields a sensitivity factor (slope) of $-6.1 \text{ W m}^{-2} \text{ K}^{-1}$, with an explained variance of 85.0%. This indicates that the net (SW + LW) radiative effect of clouds during the evolution of the composite ISO is to cool the ocean-atmosphere system during its tropospheric warm phase, and to warm it during its cool phase.

4. Discussion and Conclusions

[21] The composite of fifteen strong intraseasonal oscillations we examined revealed that enhanced radiative cool-

ing of the ocean-atmosphere system occurs during the tropospheric warm phase of the oscillation. Our measured sensitivity of total (SW + LW) cloud radiative forcing to tropospheric temperature is $-6.1 \text{ W m}^{-2} \text{ K}^{-1}$. During the composite oscillation's rainy, tropospheric warming phase, the longwave flux anomalies unexpectedly transitioned from warming to cooling, behavior which was traced to a decrease in ice cloud coverage. This decrease in ice cloud coverage is nominally supportive of Lindzen's "infrared iris" hypothesis. While the time scales addressed here are short and not necessarily indicative of climate time scales, it must be remembered that all moist convective adjustment occurs on short time scales. Since these intraseasonal oscillations represent a dominant mode of convective variability in the tropical troposphere, their behavior should be considered when testing the convective and cloud parameterizations in climate models that are used to predict global warming.

[22] **Acknowledgments.** The TMI data products are produced by Remote Sensing Systems (available at www.remss.com) and are sponsored by the NASA Earth Science REASoN DISCOVER Project. The CERES data were obtained from the NASA Langley Research Center EOSDIS Distributed Active Archive Center. The MODIS data are available at <http://ladsweb.nascom.nasa.gov/data/ftp> site.html. This research was supported by NOAA contract NA05NES4401001 and DOE contract DE-FG02-04ER63841. J. Hnilo was supported under the auspices of the DOE Office of Science, Climate Change Prediction Program by University of California Lawrence Livermore National Laboratory, contract W-7405-Eng-48.

References

- Aires, F., and W. B. Rossow (2003), Inferring instantaneous, multivariate and nonlinear sensitivities for analysis of feedbacks in a dynamical system: Lorenz model case study, *Q. J. R. Meteorol. Soc.*, *129*, 239–275.
- Barnes, W. L., T. S. Pagano, and V. V. Solomonson (1998), Prelaunch characteristics of the Moderate Resolution Imaging Spectroradiometer (MODIS) on EOS-AM1, *IEEE Trans. Geosci. Remote Sens.*, *36*, 1088–1100.
- Cess, R. D., M. Zhang, B. A. Wielicki, D. F. Young, X. Zhou, and Y. Nikitenko (2001), The influence of the 1998 El Niño upon cloud-radiative forcing over the Pacific Warm Pool, *J. Clim.*, *14*, 2129–2137.
- Chou, M.-D., and R. S. Lindzen (2002), Comments on tropical convection and the energy balance of the top of the atmosphere, *J. Clim.*, *15*, 2566–2570.
- Christy, J. R., R. W. Spencer, W. B. Norris, W. D. Braswell, and D. E. Parker (2003), Error estimates of version 5.0 of MSU/AMSU bulk atmospheric temperatures, *J. Atmos. Oceanic Technol.*, *20*, 613–629.
- Kiehl, J. T., and V. Ramanathan (1990), Comparison of cloud forcing derived from the Earth Radiation Budget Experiment with that simulated by the NCAR Community Climate Model, *J. Geophys. Res.*, *95*, 11,679–11,698.
- Kummerow, C., W. Barnes, T. Kozu, J. Shiue, and J. Simpson (1998), The Tropical Rainfall Measuring Mission (TRMM) sensor package, *J. Atmos. Oceanic Technol.*, *15*, 809–817.
- Lindzen, R. S., M.-D. Chou, and A. Y. Hou (2001), Does the Earth have an adaptive infrared iris?, *Bull. Am. Meteorol. Soc.*, *82*, 417–432.
- Madden, R. A., and P. R. Julian (1994), Observations of the 40–50 day tropical oscillation: A review, *Mon. Weather Rev.*, *122*, 814–837.
- Manabe, S., and R. F. Strickler (1964), Thermal equilibrium of the atmosphere with a convective adjustment, *J. Atmos. Sci.*, *21*, 361–385.
- Soden, B. J., and I. M. Held (2006), An assessment of climate feedbacks in coupled ocean-atmosphere models, *J. Clim.*, *19*, 3354–3360.
- Spencer, R. W., and W. D. Braswell (1997), How dry is the tropical free troposphere? Implications for global warming theory, *Bull. Am. Meteorol. Soc.*, *78*, 1097–1106.
- Stephens, G. L. (2005), Cloud feedbacks in the climate system: A critical review, *J. Clim.*, *18*, 237–273.
- Stephens, G. L., P. Webster, R. Johnson, R. Engelen, and T. L'Ecuyer (2004), Observational evidence for the mutual regulation of the tropical hydrological cycle and tropical sea surface temperatures, *J. Clim.*, *17*, 2213–2224.
- Wentz, F. (1997), A well-calibrated ocean algorithm for the Special Sensor Microwave/Imager, *J. Geophys. Res.*, *102*, 8703–8718.

- Wentz, F. J., and R. W. Spencer (1998), SSM/I rain retrievals within a unified all-weather ocean algorithm, *J. Atmos. Sci.*, *55*, 1613–1627.
- Wentz, F., C. Gentemann, and D. Smith (2000), Satellite measurements of sea surface temperature through clouds, *Science*, *288*, 847–850.
- Wielicki, B. A., B. R. Barkstrom, E. F. Harrison, R. B. Lee III, G. L. Smith, and J. E. Cooper (1996), Clouds and the Earth's Radiant Energy System (CERES): An Earth Observing System experiment, *Bull. Am. Meteorol. Soc.*, *77*, 853–868.
-
- W. D. Braswell, J. R. Christy, and R. W. Spencer, Earth System Science Center, 320 Sparkman Drive, University of Alabama in Huntsville, Huntsville, AL 35801, USA. (roy.spencer@nssc.uah.edu)
- J. Hnilo, Lawrence Livermore National Laboratory, 7000 East Avenue, Livermore, CA 94550, USA.

EXHIBIT 193

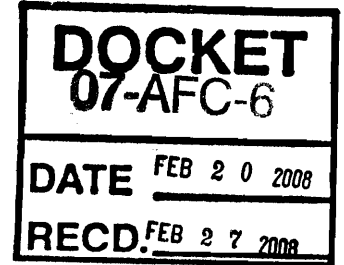


City of Carlsbad

Office of the City Manager

February 20, 2008

Michael Monasmith
Project Manager, Siting Division
California Energy Commission
1516 Ninth Street
Sacramento, CA 95814



Clarification to California Energy Commission on Carlsbad Municipal Water District Projected Reclaimed Water Supply (07-AFC-6)

Dear Mr. Monasmith:

There has been significant discussion regarding the availability of reclaimed water to support the proposed Carlsbad Energy Center Project (07-AFC-6), which is currently under review.

The City of Carlsbad would like to submit the following overview of Carlsbad's reclaimed water supply for the Commission's information. All units of water are shown in either million gallons per day (mgd) or acre feet per month (afm). An operational factor of 95% peak capacity was applied in calculating the estimated gross afm production.

Water Supply

The City of Carlsbad currently has three sources of reclaimed water, which are:

- Carlsbad Water Recycling Facility (CWRF)
- Meadowlark Water Reclamation Facility (MWRF)
- Gaffner Water Reclamation Facility (GWRF)

CWRF

The CWRF is the only City-owned facility and represents the bulk of production capacity. The CWRF was constructed as part of the City's desire to increase its recycled water capacity. This \$45 million expansion has been ongoing since 2000 and is expected to achieve full production by 2012. CWRF has a peak production capacity of 4 mgd, or approximately 350 afm.



MWRF

The MWRF is owned and operated by Vallecitos Water District. MWRF is currently being expanded and, when operational (expected online date summer 2008), the City will increase its peak contracted capacity from 2 mgd (174 afm) to 3 mgd (261 afm). The contract between the City and Vallecitos terminates in 2025. Water from the MWRF helps supply the entire Carlsbad reclaimed water system.

GWRF

The City contracts with the Leucadia Wastewater District to receive approximately 750,000 gallons per day (70 afm). Water from GWRF is used solely to supply the La Costa Golf Course's south course through a separate delivery system. It should be noted that the City is unable to use this water in the larger system, as there does not exist a direct connection between Carlsbad and GWRF. The contract is set to expire in 2011, and the City is not anticipating its renewal at this time.

Overall Supply Picture

The City of Carlsbad currently has 6.75 mgd of peak production capacity (594 afm) with an anticipated increase to 7.75 mgd (681 afm) once improvements to MWRF are complete. With the expiration of the GWRF contract in 2011, system capacity is projected to be reduced back to 7 mgd (611 afm). The chart below outlines the City's projected reclaimed water supply in available acre feet per month, based on 95% peak production capacity.

Source of Supply	Quantity of Supply		
	<u>2007</u>	<u>2010</u>	<u>2012</u>
CWRF	350 afm	350 afm	350 afm
MWRF	174 afm*	261 afm	261 afm
GWRF	70 afm	70 afm	-
Total Supply	594 afm	681 afm	611 afm

*Reclaimed water not available due to construction

Water Demand

The City of Carlsbad currently has approximately 215 recycled water customers who receive water through more than 430 metered connections. Recycled water demand, as consistent with potable water demand, is seasonal in nature. Although the City currently has capacity to meet existing customer needs, the projected peak demand (790 afm) will begin to exceed supply by 2009. This increased demand is projected to grow through 2014 and will result in the City being unable to meet its full reclaimed water needs during peak months (May-September) with existing supply and storage infrastructure (the City has use of a 54-million gallon reservoir to help meet peak demand).

The attached spreadsheet outlines the City's supply and demand projections through 2014. Months where demand exceeds supply are shown in red. Included in the attached spreadsheet is the projected impact of supplying the proposed Carlsbad Energy Center Project.

Summary

The City of Carlsbad has been actively developing its reclaimed water system for the past decade. These system improvements are anticipated to be fully realized over the next several years, at which time, peak demand for reclaimed water is predicted to exceed monthly production capacity.

Should you have any questions regarding the City's reclaimed water system, please contact me at (760) 434-2820 or jgaru@ci.carlsbad.ca.us.

Sincerely,



Joe Garuba
Municipal Projects Manager
City of Carlsbad

c: Tim Hemig, Carlsbad Energy Center, LLC
John A. McKinsey, Stoel Rives, LLP
Lisa Hildabrand, Interim City Manager
Ron Ball, City Attorney
Jim Elliott, Deputy City Manager
Glenn Pruim, Public Works Director
Debbie Fountain, Housing and Redevelopment Director
Scott Donnell, Senior Planner

**Carlsbad Municipal Water District
Projected Reclaimed Water Supply vs. Demand**

Month	Supply	Demand	Difference	CECP	Difference
July	420	418.0	2.0		
August	420	366.7	53.3		
September	420	397.8	22.2		
October	420	366.1	53.9		
November	420	280.1	139.9		
December	420	69.2	350.8		
January	420	67.9	352.1		
February	420	140.0	280.0		
March	420	160.0	260.0		
April	420	190.0	230.0		
May	420	250.0	170.0		
June	420	350.0	70.0		
FY 07/08 Total	5040	3,055.80			

Month	Supply	Demand	Difference	CECP	Difference
July	681	672.0	9.0		
August	681	563.0	118.0		
September	681	483.0	198.0		
October	681	348.0	333.0		
November	681	134.0	547.0		
December	681	147.0	534.0		
January	681	35.0	646.0		
February	681	51.0	630.0		
March	681	118.0	563.0		
April	681	262.0	419.0		
May	681	438.0	243.0		
June	681	585.0	96.0		
FY 08/09 Total	8172	3,836.00			

Month	Supply	Demand	Difference	CECP	Difference
July	681	790.0	(109.0)		
August	681	662.0	19.0		
September	681	568.0	113.0		
October	681	410.0	271.0		
November	681	158.0	523.0		
December	681	173.0	508.0		
January	681	41.0	640.0		
February	681	60.0	621.0		
March	681	139.0	542.0		
April	681	308.0	373.0		
May	681	515.0	166.0		
June	681	688.0	(7.0)		
FY 09/10 Total	8172	4,512.00	3660.0		

Month	Supply	Demand	Difference	CECP	Difference
July	681	920.0	(239.0)	93.3	(332.3)
August	681	771.0	(90.0)	93.3	(183.3)
September	681	661.0	20.0	93.3	(73.3)
October	681	477.0	204.0	0	204.0
November	681	184.0	497.0	0	497.0
December	681	201.0	480.0	0	480.0
January	681	48.0	633.0	0	633.0
February	681	70.0	611.0	0	611.0
March	681	162.0	519.0	0	519.0
April	611	359.0	252.0	0	252.0
May	611	600.0	11.0	93.3	(82.3)
June	611	801.0	(190.0)	93.3	(283.3)
FY 10/11 Total	7962	5,254.00	2708.0		

Month	Supply	Demand	Difference	CECP	Difference
July	611	962.0	(351.0)	93.3	(444.3)
August	611	806.0	(195.0)	93.3	(288.3)
September	611	691.0	(80.0)	93.3	(173.3)
October	611	499.0	112.0	0	112.0
November	611	192.0	419.0	0	419.0
December	611	210.0	401.0	0	401.0
January	611	50.0	561.0	0	561.0
February	611	73.0	538.0	0	538.0
March	611	169.0	442.0	0	442.0
April	611	375.0	236.0	0	236.0
May	611	627.0	(16.0)	93.3	(109.3)
June	611	838.0	(227.0)	93.3	(320.3)
FY 11/12 Total	7332	5,492.00	1840.0		

Month	Supply	Demand	Difference	CECP	Difference
July	611	1000.0	(389.0)	93.3	(482.3)
August	611	838.0	(227.0)	93.3	(320.3)
September	611	719.0	(108.0)	93.3	(201.3)
October	611	519.0	92.0	0	92.0
November	611	200.0	411.0	0	411.0
December	611	219.0	392.0	0	392.0
January	611	52.0	559.0	0	559.0
February	611	76.0	535.0	0	535.0
March	611	176.0	435.0	0	435.0
April	611	390.0	221.0	0	221.0
May	611	652.0	(41.0)	93.3	(134.3)
June	611	871.0	(260.0)	93.3	(353.3)
FY 12/13 Total	7332	5,712.00	1620.0		

Month	Supply	Demand	Difference	CECP	Difference
July	611	1046.0	(435.0)	93.3	(528.3)
August	611	877.0	(266.0)	93.3	(359.3)
September	611	752.0	(141.0)	93.3	(234.3)
October	611	542.0	69.0	0	69.0
November	611	209.0	402.0	0	402.0
December	611	229.0	382.0	0	382.0
January	611	55.0	556.0	0	556.0
February	611	80.0	531.0	0	531.0
March	611	184.0	427.0	0	427.0
April	611	408.0	203.0	0	203.0
May	611	682.0	(71.0)	93.3	(164.3)
June	611	912.0	(301.0)	93.3	(394.3)
FY 13/14 Total	7332	5,976.00	1356.0		

All quantities are in acre feet per month (AF/per month).

Supply is calculated on a 95% operational factor based on peak mgd capacity

93.3 AF/Per month = 1 million gallons per day (mgd)

700 gpm = 1 mgd

The CECP is projected at 700 gallons per minute (GPM) in peak months (May-September). This is = to 40% operating time

Projected CECP online date Summer 2010

BEFORE THE ENERGY RESOURCES CONSERVATION AND DEVELOPMENT
COMMISSION OF THE STATE OF CALIFORNIA
1516 NINTH STREET, SACRAMENTO, CA 95814
1-800-822-6228 – WWW.ENERGY.CA.GOV

APPLICATION FOR CERTIFICATION
FOR THE CARLSBAD ENERGY
CENTER PROJECT

Docket No. 07-AFC-6
PROOF OF SERVICE
(Revised 1/27/2010)

**Carlsbad Energy Center LLC's
Re Applicant's Request to Add Exhibits to Applicant's Rebuttal Testimony**

CALIFORNIA ENERGY COMMISSION
Attn: Docket No. 07-AFC-6
1516 Ninth Street, MS-4
Sacramento, CA 95814-5512
docket@energy.state.ca.us

INTERESTED AGENCIES

California ISO
P.O. Box 639014
Folsom, CA 95763-9014
(e-mail preferred) e-recipient@caiso.com

APPLICANT

David Lloyd
Carlsbad Energy Center, LLC
1817 Aston Avenue, Suite 104
Carlsbad, CA 92008
David.Lloyd@nrqenergy.com

INTERVENORS

City of Carlsbad
South Carlsbad Coastal Redevelopment Agency
Allan J. Thompson
Attorney for City
21 "C" Orinda Way #314
Orinda, CA 94563
allanori@comcast.net

George L. Piantka, PE
Carlsbad Energy Center LLC
1817 Aston Avenue, Suite 104
Carlsbad, CA 92008
george.piantka@nrqenergy.com

City of Carlsbad
South Carlsbad Coastal Redevelopment Agency
Joseph Garuba, Municipals Project Manager
Ronald R. Ball, Esq., City Attorney
1200 Carlsbad Village Drive
Carlsbad, CA 92008 (e-mail preferred)
Joe.Garuba@carlsbadca.gov;
ron.ball@carlsbad.ca.gov

APPLICANT'S CONSULTANTS

Robert Mason, Project Manager
CH2M Hill, Inc.
6 Hutton Centre Drive, Ste. 700
Santa Ana, CA 92707
Robert.Mason@ch2m.com

Terramar Association
Kerry Siekmann & Catherine Miller
5239 El Arbol
Carlsbad, CA 92008
siekmann1@att.net

Megan Sebra
CH2M Hill, Inc.
2485 Natomas Park Drive, Ste. 600
Sacramento, CA 95833
Megan.Sebra@ch2m.com

California Unions for Reliable Energy ("CURE")
Gloria D. Smith & Marc D. Joseph
Adams Broadwell Joseph & Cardozo
601 Gateway Boulevard, Suite 1000
South San Francisco, CA 94080
gsmith@adamsbroadwell.com
mdjoseph@adamsbroadwell.com

COUNSEL FOR APPLICANT

John A. McKinsey
Stoel Rives LLP
500 Capitol Mall, Ste. 1600
Sacramento, CA 95814
jamckinsey@stoel.com

INTERVENORS

ENERGY COMMISSION

Center for Biological Diversity
c/o William B. Rostove
EARTHJUSTICE
426 17th St., 5th Floor
Oakland, CA 94612
wrostov@earthjustice.org

Power of Vision
Julie Baker and Arnold Roe, Ph.D.
4213 Sunnyhill Drive
Carlsbad, CA 92008-3647
powerofvision@roadrunner.com

Rob Simpson
Environmental Consultant
27126 Grandview Avenue
Hayward, CA 94542
rob@redwoodrob.com

JAMES D. BOYD
Vice Chair and Presiding Member
jboyd@energy.state.ca.us

ANTHONY EGGERT
Commissioner and Associate Member
aeggert@energy.state.ca.us

Paul Kramer
Hearing Office
pkramer@energy.state.ca.us

Mike Monasmith
Siting Project Manager
mmonasmi@energy.state.ca.us

Dick Ratliff
Staff Counsel
dratliff@energy.state.ca.us

Public Adviser's Office
publicadviser@energy.state.ca.us

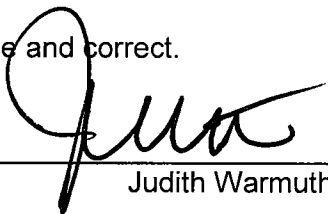
DECLARATION OF SERVICE

I, Judith Warmuth, declare that on January 29, 2010, I deposited copies of the aforementioned document in the United States mail at 500 Capitol Mall, Suite 1600, Sacramento, California 95814, with first-class postage thereon fully prepaid and addressed to those identified on the Proof of Service list above.

OR

Transmission via electronic mail was consistent with the requirements of California Code of Regulations, Title 20, sections 1209, 1209.5, and 1210. All electronic copies were sent to all those identified on the Proof of Service list above.

I declare under penalty of perjury that the foregoing is true and correct.



Judith Warmuth